Journal of Zhejiang University-SCIENCE A (Applied Physics & Engineering)
ISSN 1673-565X (Print); ISSN 1862-1775 (Online)
www.zju.edu.cn/jzus; www.springerlink.com
E-mail: jzus@zju.edu.cn

# An examination of the mechanical interaction of drilling slurries at the soil-concrete contact*

Ressol R. SHAKIR†[1,2], Jun-gao ZHU[1,2]

([1]*Key Laboratory of MOE for Geomechanics and Embankment Engineering, Hohai University, Nanjing 210098, China*)

([2]*Geotechnical Research Institute, Hohai University, Nanjing 210098, China*)

†E-mail: rrshakir@yahoo.com

Received July 26, 2009; Revision accepted Nov. 9, 2009; Crosschecked Jan. 6, 2010

**Abstract:** Evidence gained from previous field tests conducted on drilled shaft foundation shows that using drilling slurries to stabilize a borehole during the construction may influence the interfacial shear strength. This paper deals with an exhaustive study of the effects of drilling slurries at the contact between soil and concrete. This study involved adapting a simple shear apparatus and performing approximately 100 experimental tests on the interaction between two types of soils; clay and sandy clay and five specimens of concrete with different surface shapes. It also involved using bentonite and polymer slurries as an interface layer between soil and concrete. Results showed that an interface layer of bentonite slurry between clay and concrete decreases the interfacial shear strength by 23% and as an interface layer between sandy clay and concrete, bentonite increases interfacial shear strength by 10%. Using polymer slurry as an interface layer between clay and concrete decreases the interfacial shear strength by 17% while using it as an interface layer between sandy clay and concrete increases the interfacial shear strength by 10%. Furthermore, the data show that using bentonite and polymer slurry as an interface layer between clay and concrete decreases the sliding ratio by 50% to 60%, while increasing the sliding ratio by 44% to 56% when these are used as an interface layer between sandy clay and concrete.

**Key words:** Drilled shaft foundation, Drilling slurry, Polymer, Bentonite, Simple shear test, Concrete surface, Soil structure interaction, Mudcake

**doi:**10.1631/jzus.A0900456 **Document code:** A **CLC number:** TU4

## 1 Introduction

Constructing drilled shaft foundation sometimes requires various types of drilling slurries to stabilize the borehole. These slurries are generally divided into two groups: the mineral slurries and the polymer slurries. Using a slurry mixture may cause loss of friction because slurry residual settling may lead to the development of thick membranes of weak material (mudcake) at both the sides and bottom of borehole.

Many researchers have investigated the effect of mudcake on the pile load transfer and the factors influencing mudcake formation. These factors include roughness, exposure time, hydrostatic of slurry column, and all affect the thickness layer and side resistance (Cernak, 1973; Pells *et al*., 1978; Nash, 1974; Wates and Knight, 1975; Holden, 1984; O'Neill and Hassan, 1994). Some studies have concentrated on the effects of soil type on the pile load transfer (Tucker and Reese, 1984; Majano *et al*., 1994). Majano *et al*. (1994) reported that slurry penetrates the soil, that filtration of bentonite platelets occurs, and that thixotropic gel forms on the surface of mudcake, which becomes thicker and more impermeable with time.

Advances in technology have led to polymer slurries as new materials to be used in stabilizing boreholes, a prospect that has attracted great attention

* Project supported by the National Natural Science Foundation of China (No. 50639050), and the China Scholarship Council (No. 2006368T15)

in the last two decades. The semisynthetic polymers most commonly used are anionic polyacrylamides (AP) and vinyls that are soluble in water and which are able to form long hydrocarbon chains when exposed to water (Majano *et al.*, 1993). In general, the field research on polymer slurries mainly deals with two matters: the ability of polymer slurry to stabilize the borehole and the effect of polymer slurry on the perimeter load transfer. Studies have shown that polymer successfully stabilizes the borehole through construction drilled shafts and increases the load transfer (Kheng, 1989; Majano *et al*., 1994; Ata and O'Niell, 2000).

The main cause of a reduced bearing capacity when using drilling slurry is the existence of thick mudcake, which reduces the side resistance by lessening the bond between hole sides and concrete. Some reports have shown that this is not an issue when the mudcake is not excessive (O'Neill and Reese, 1999; Camp *et al*., 2002). Another report has shown that bentonite reduces the side resistance even with thin mudcake produced by exposing the hole for slurry for short time (Brown, 2002).

Most of the above-mentioned studies used large-scale field tests. Although they presented valuable conclusions, the approach is not adaptable to conducting multiple tests and is expensive. Direct shear and simple shear tests for comprehensive soil structure interface applications are more practical than large-scale tests and considered optimal for detailed studies.

Some researchers have used a simple shear apparatus to study the friction between soil and steel plates and between soil and concrete (Uesugi *et al*., 1990; Tsubakihara *et al*., 1993; Wang and Lu, 2007). Large scale direct shear apparatus have been used to study the interface between soil and concrete and also between gravel-containing soil and steel plate (Yin *et al*., 1995; Zhang and Zhang, 2009). Zhang *et al*. (2008) used a large simple shear apparatus to explore the mechanical behavior of the interface between core and filter soils in rock fill dams. Shakir and Zhu (2009) used a simple shear apparatus to study the interface between compacted clay and concrete. Recently, a direct shear apparatus was used to study concrete-rock interface and sand-steel interface (Reddy *et al*., 2000; Xue *et al*., 2005; Jeong *et al*., 2009). Laboratory experimental tests to examine the effect of thin layer slurries between soil and concrete are few and need more investigation.

In this study, a simple shear apparatus capable of measuring the sliding and deformation displacement in split form was modified and used to study the soil structure interface. The main objectives were: (1) to explore the effect of using bentonite slurry and polymer slurry as an interface layer between two types of soils (clay and sandy clay) and five specimens of concrete with different surface shape; and (2) to derive a method for analyzing the sliding and deformation displacement obtained from simple shear tests.

## 2 Simple shear apparatus and tested materials

### 2.1 Simple shear apparatus

Fig. 1 shows a schematic view of the interface simple shear apparatus used in this study. Originally, the Geotechnical Research Institute in Hohai University, China designed this apparatus to test soil structure interfaces. In the present study, we adapted the simple shear apparatus and used it to test the interface between soil and concrete under monotonic loading. Adapting the apparatus involved using Global Digital Systems (GDS) standard pressure/volume controller to apply controlled shear force. A proving ring-based dial gauge was used to measure the applied shear force. The GDS was used for triaxial testing and has been used recently for direct shear tests (Zhu and Yin, 2001; Barla *et al*., 2007).

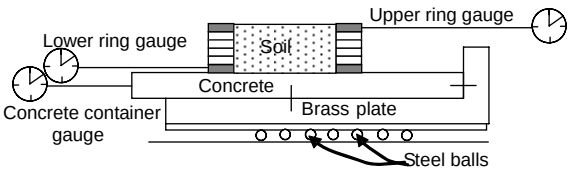


**Fig. 1 Schematic view of the simple shear apparatus**

All gauges were linked to a computer which used modified software to record dial gauge readings during the tests. Containers with inner size 107 mm× 107 mm were made and filled by concrete mortar. The contact area between clay and concrete does not change (since the concrete area is greater than contact area of the clay sample even when sliding displace-

ment occurs). A stack of rings made from copper with diameter of 60 mm represents the container of sample. Minimization of the friction induced between rings required lubricating them to allow free occurrence of clay mass deformation. The height of the sample was 10 mm. Normal displacement was measured by strain gauge with accuracy 0.001 mm/digit, the same type being used for tangential displacement.

### 2.2 Computing sliding and deformation displacement

Calculating tangential displacement requires the readings of three gauges located at the concrete container, at the lower and upper rings of container rings (Fig. 1). Fig. 2 shows a schematic diagram for the method of calculation the sliding and deformation displacement because of shear stress application. Sliding displacement is the difference between the displacement of bottom ring (which is located in contact with the concrete) and the displacement of concrete, i.e., $d_s=d_c-d_l$. Subtraction of the sliding displacement from the displacement of the top ring of the sample container is the deformation displacement ($d_d=d_l-d_u$). Total displacement is calculated by adding sliding displacement to deformation displacement ($d_t=d_s+d_d$). Thus, in a simple shear test, displacement can be split into two components: shear sliding displacement and shear deformation displacement, an approach which increases the ability to understand interface behavior.

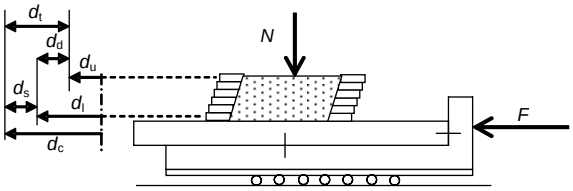


**Fig. 2 Schematic view of sliding, deformation, and total shear displacement**

$d_t$: total displacement; $d_d$: deformation displacement; $d_s$: sliding displacement; $d_u$: upper ring displacement; $d_l$: lower ring displacement; $d_c$: concrete-plate displacement

### 2.3 Structural material

Preparing concrete material involved obtaining a practical compression strength and repeatedly testing with minimum wear in the concrete surface. Five containers were made to pour the concrete mortar. These containers consisted of four pieces welded to a plate at the bottom face. The concrete containers minimized the deformation in concrete. They were fastened by bolds to another brass plate which moved on sliding steel balls. The concrete was prepared by mixing the sand and cement with 60% water-cement ratio (w/c), and then the five containers were filled by the concrete mortar. The weight ratio of cement to sand (c:s) was 1:2.5. Scratch was used to fill the concrete mortar into concrete containers and spatula was used to end the surface. The outer dimensions of each container were 150 mm×115 mm×40 mm. Using the five containers of concrete in the interface testing program required embedding them under wet sand for at least 28 d. The compressive strength for concrete samples was 23 MPa.

Fig. 3 shows pictures of a 2.0 cm×1.5 cm concrete specimens with different surface shapes using a spatula. These pictures represent five surface shapes: #1 smooth shape, #2 horizontal lines shape, #3 random shape, #4 inclined lines shape and #5 network lines shape.

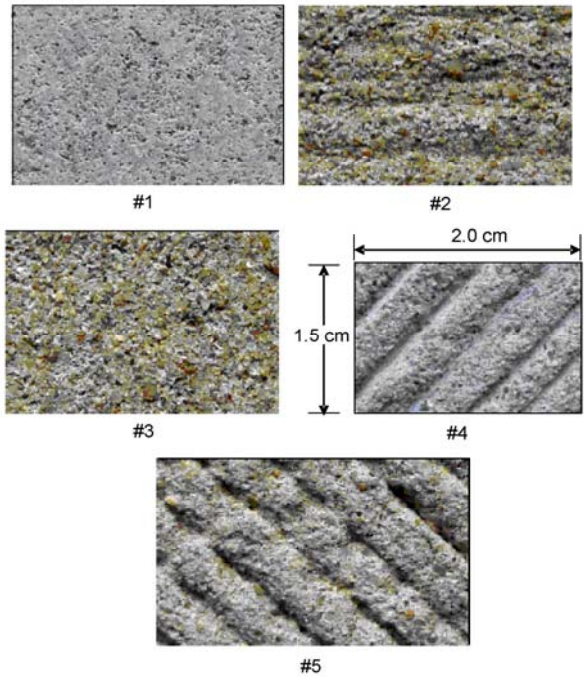


**Fig. 3 Concrete surface shapes**

### 2.4 Soil and slurry samples preparing

The experimental study considered two types of soils clay and sandy clay. The main properties of clay such as plastic limit ($l_p$), liquid limit ($l_l$), plastic index ($l_{pi}=l_l-l_p$) and specific gravity ($G_s$) are summarized in Table 1. The dry density of clay is 1.65 g/cm$^3$ and the optimum water content is about 18%.

**Table 1 Main properties of clay**

| $l_l$ | $l_p$ | $l_{pi}$ | $G_s$ | $\rho_d$ | $W_c$ |
|---|---|---|---|---|---|
| 35.08 | 19.98 | 15.1 | 2.68 | 1.65 | 18% |

For the sand, the dry density is 1.9 g/cm$^3$ and the optimum water content is about 12%. Table 2 shows the properties of sand such as the diameter opposite to 10%, 30% and 60% finer ($D_{10}$, $D_{30}$, $D_{60}$) as well as the coefficient of uniformity ($C_u$) and coefficient of curvature ($C_c$). Sandy clay soil was made by mixing 75% sand and 25% clay. The sample was prepared by compacting soil inside the container of rings with a constant dry density.

**Table 2 Sand soil properties**

| $D_{10}$ (mm) | $D_{30}$ (mm) | $D_{60}$ (mm) | $C_u=\frac{D_{60}}{D_{10}}$ | $C_c=\frac{D_{30}^2}{D_{60}D_{10}}$ |
|---|---|---|---|---|
| 0.16 | 0.3 | 0.45 | 2.8 | 1.25 |

Preparing bentonite slurry required mixing small quantities of bentonite powder with water and waiting for 4 h for hydration. Testing required placing a thin layer of bentonite slurry on the sample by the spatula, then placing the sample on the concrete after 5 min. The final step was to apply constant normal loading and shear force.

Drilling shaft anionic polyacrylamide polymer is available commercially in the form of small particles packed in small tins of about 400 g. Preparation of the sample of polymer slurry involved mixing 1 g of solid particles with 1 L of water. The polymer slurry can be used within minutes because no hydration occurs. A thin film (1 mm) of polymer slurry between soil and concrete is then made.

## 3 Results and discussion

The laboratory test program involves carrying out experimental tests with six groups of materials. They are clay concrete interface (CCI), clay-bentonite slurry-concrete interface (CBCI), clay-polymer slurry -concrete interface (CPCI), sandy clay concrete interface (SCCI), sandy clay-bentonite slurry-concrete interface (SCBCI), and sandy clay-polymer slurry-concrete interface (SCPCI). For each group, plan of research involved conducting the tests with five types of concrete surface shape. Normal stresses ranged from 52 to 400 kPa for soil concrete interface without bentonite or polymer slurry at interface and ranged from 52 to 204 kPa for the bentonite and polymer slurry interface.

The simple shear test revealed three types of relations: shear stress vs. total shear displacement, vertical displacement vs. total displacement, and sliding displacement vs. deformation displacement. Approximately 100 experiments were involved. Because of space limitations, only the results of SCBCI (#3) are presented (#3 refers to a concrete specimen type #3).

### 3.1 Stress displacement relations

The shear strength increases with increase in normal stress ($\sigma_n$) intensity (Fig. 4a), producing about 80 kPa for normal stress 204 kPa, and 15 kPa for normal stress 52 kPa. Generally, the shape of the curve is hyperbolic. Normal displacement also displays different values with different normal stresses, for $\sigma_n$=204 kPa, $w$=0.61 mm (Fig. 4b), where $w$ is the normal displacement.

Among the three curves of $d_s$ vs. $d_d$ relation, the

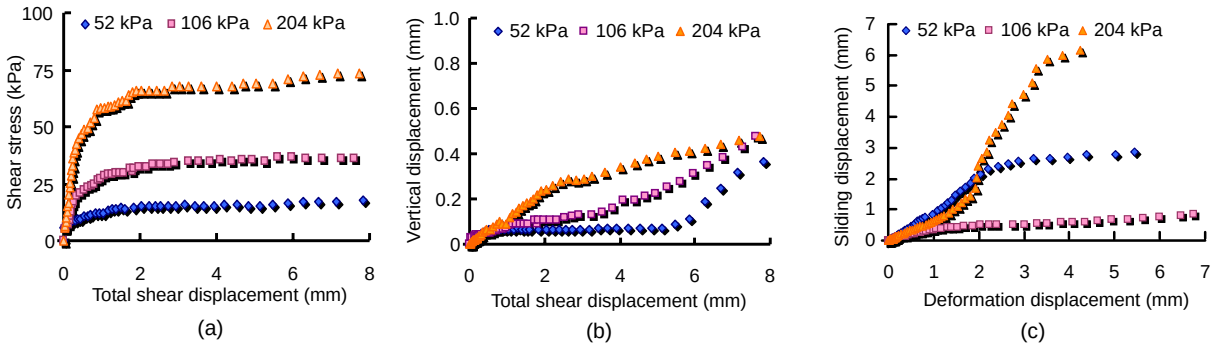


**Fig. 4 Relation between (a) interface shear stress and total shear displacement for SCBCI (#3), (b) total shear displacement and vertical displacement for SCBCI (#3), and (c) deformation and sliding displacement for SCBCI (#3)**

curve of $\sigma_n$=204 kPa shows the greatest sliding displacement ($d_s$=6.1 mm) (Fig. 4c). The sliding displacement is also greater than deformation displacement ($d_s$>$d_d$, $d_d$=4.2 mm) for the same normal stress. As normal stress intensity is changed, displacement, whether it is deformation or sliding, is also changed. For $\sigma_n$=106 kPa, $d_s$=2.8 mm, $d_d$=5.4 mm, and for $\sigma_n$ =52 kPa, $d_s$=0.9 mm, $d_d$=6.8 mm. Increasing sliding displacement indicates a failure in the contact surface between soil and concrete. The average value for deformation displacement is 5.5 mm and for sliding displacement is 3.3 mm.

### 3.2 Maximum interfacial shear strength

Fig. 5 shows the maximum interfacial shear strength and normal stress for clay concrete interface (CCI). All the obtained-relations between interfacial shear strength and normal stress show a nearly linear response. The concrete surface shape affects the results of the interface. It is expected that a smooth surface will give a low angle of friction in comparison to the rough surfaces. Tests of interface between clay and concrete of a smooth surface type (i.e., CCI (#1)) reveal the lowest value of interface shear strength, $\tau$ =290 kPa, when normal stress is 400 kPa, in comparison to other surfaces. Tests of interface between clay and concrete of the rough surface (i.e., CCI (#4)) show the highest value, $\tau$=290 kPa of maximum interface shear strength for the same normal stress.

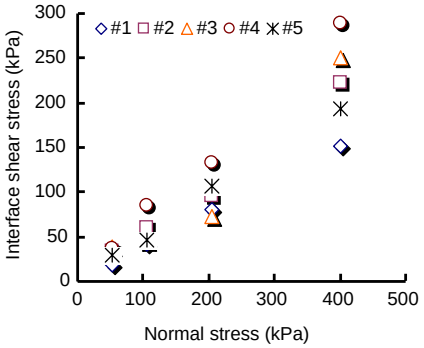


**Fig. 5 Maximum shear stress vs. normal stress for CCI**

Two parameters obtained from fitting line of relation between $\tau^{max}$ and $\sigma_n$ are the cohesion ($C$) and the angle of friction ($\delta$). In the following sections, discussion will focus on $C$ and $\delta$ as well as the maximum interfacial shear strength.

### 3.3 Drilling slurries and soil type effects

Using bentonite slurry as an interface layer between soil and concrete lessens the angle of friction, and increases the cohesion, but the interfacial shear strength decreases by 23%, $(\tau^{av}_{CBCI}-\tau^{av}_{CCI})/\tau^{av}_{CCI}$ =0.23 (Table 3). Here $\tau^{av}_{CBCI}$ and $\tau^{av}_{CCI}$ are calculated by taking the average for maximum shear stresses obtained by applying the Mohr-Coulomb equation ($\tau^{max}=C^{av}+\sigma_n\tan\delta^{av}$) for the parameters $C^{av}$ and $\delta^{av}$ (Table 3) using three normal stresses (150 kPa, 106 kPa, and 204 kPa). Average value of angle of friction ($\delta^{av}$) for CCI is 28.5° and it equals 19.3° when the layer of bentonite was used between soil and concrete (CBCI). Cohesion increased from 0.5 to 9.0 kPa.

Using a bentonite layer between sandy clay and concrete shows contrasting results. The bentonite increases the average of angle of friction $\delta^{av}$, decreases the cohesion, however, the interfacial shear strength increases by 10%. $\delta^{av}$ for the example without bentonite is 13.0° while using bentonite make $\delta^{av}$ equal 20.2° (Table 4). Cohesion decreases from 12.9 kPa for SCCI to 0.4 kPa for SCBCI.

**Table 3 Angle of friction and cohesion for CCI, CBCI and CPCI interfaces**

| Concrete type | $C$ | | | $\delta$ (°) | | |
|---|---|---|---|---|---|---|
| | CCI | CBCI | CPCI | CCI | CBCI | CPCI |
| #1 | 0.7 | 0.0 | 0.0 | 20.8 | 15.9 | 24.2 |
| #2 | 0.0 | 3.3 | 10.8 | 28.4 | 20.1 | 26.1 |
| #3 | 0.0 | 6.8 | 18.6 | 32.3 | 18.9 | 18.3 |
| #4 | 0.5 | 21.6 | 34.4 | 35.4 | 19.7 | 11.3 |
| #5 | 1.4 | 13.5 | 6.12 | 25.8 | 22.1 | 14.6 |
| av. | 0.5 | 9.0 | 14.0 | 28.5 | 19.3 | 18.9 |

**Table 4 Angle of friction and cohesion for SCCI, SCBCI and SCPCI interfaces**

| Concrete type | $C$ | | | $\delta$ (°) | | |
|---|---|---|---|---|---|---|
| | SCCI | SCBCI | SCPCI | SCCI | SCBCI | SCPCI |
| #1 | 4.5 | 0.0 | 6.6 | 14.2° | 19.8° | 19.4° |
| #2 | 14.1 | 0.0 | 1.5 | 13.1° | 19.1° | 19.4° |
| #3 | 15.0 | 0.0 | 10.4 | 13.0° | 20.9° | 16.7° |
| #4 | 16.6 | 1.8 | 5.3 | 13.4° | 20.6° | 19.7° |
| #5 | 14.1 | 0.0 | 6.1 | 11.5° | 20.7° | 14.8° |
| av. | 12.9 | 0.4 | 6.0 | 13.0° | 20.2° | 18.0° |

Using polymer slurry between clay and concrete leads to a decrease in the average angle of friction. For example, for CPCI, $\delta^{av}$ equals 18.9° and for CCI it equals 28.5°, cohesion increasing from 0.5 kPa for CCI to 14.0 kPa for CPCI. The decrease in interfacial shear strength, however, is about 17% where $(\tau^{av}_{CPCI}-\tau^{av}_{CCI})/\tau^{av}_{CCI}=0.17$. The decrease in interfacial shear strength for a CPCI of 17% is less than that of bentonite (23%). For SCPCI, the average angle of friction increased from 13.0 for SCCI to 18.0, and cohesion decreased from 12.9 for SCCI to 6.0. There was, however, an increase in the interfacial shear strength by 10% where $(\tau^{av}_{SCPCI}-\tau^{av}_{SCCI})/\tau^{av}_{SCCI}$=0.1.

The type of soil plays an important role in increasing interfacial shear strength or lessening interfacial shear strength when slurry was used as an interface layer between soil and concrete (Tables 3 and 4). For CCI, either of the two slurries used in this study (bentonite or polymer) reduced the angle of friction by 17% to 23%. For SCCI, using bentonite slurry or polymer slurry increases the interfacial shear strength by 10%.

### 3.4 Roughness effect

The roughness of concrete surface was determined using image processing techniques and the Fast Fourier transformation tool for three specimens of concrete (#2, #3 and #4). A number of experiments used a camera with a resolution 512×512 pixels and a projector linked to optic source to get 3D images. Three images show the surface roughness (Fig. 6). The original source for this method is Takeda and Mutoh (1983). Recently, Huang *et al.* (2009) discussed methods of this type of analysis as well.

At least 25 lines are selected randomly from each image. For each line, the difference between the highest peak and the lowest valley ($R_{max}$) is calculated. The average of the highest distance between the peak and valley in the image represents the degree of roughness ($R$). The degree of roughness is normalized by dividing the average degree of roughness by the thickness of the sample (10 mm), i.e., $R_{max}$/10. Roughness degrees of three types of concrete #2, #3, and #4 are 0.25, 0.45, 0.36, respectively. Some points in the images are ignored because they form extreme values related to image distortion.

Roughness affects the angle of friction in different ways. For CCI, the linear response shows an increase in the angle of friction with the roughness degree by 19.75$R$ and for CBCI shows a decrease by 5.72$R$ (Fig. 7). For CPCI, the linear response shows a dramatic decrease in the angle of friction by 39.66$R$. The cohesion slightly increases with roughness by 0.1$R$ for CCI, by 20.20$R$ for CBCI, and by 41.48$R$ for CPCI (Fig. 8). The cohesion increases because the bentonite and polymer behave as bond material between clay and concrete.

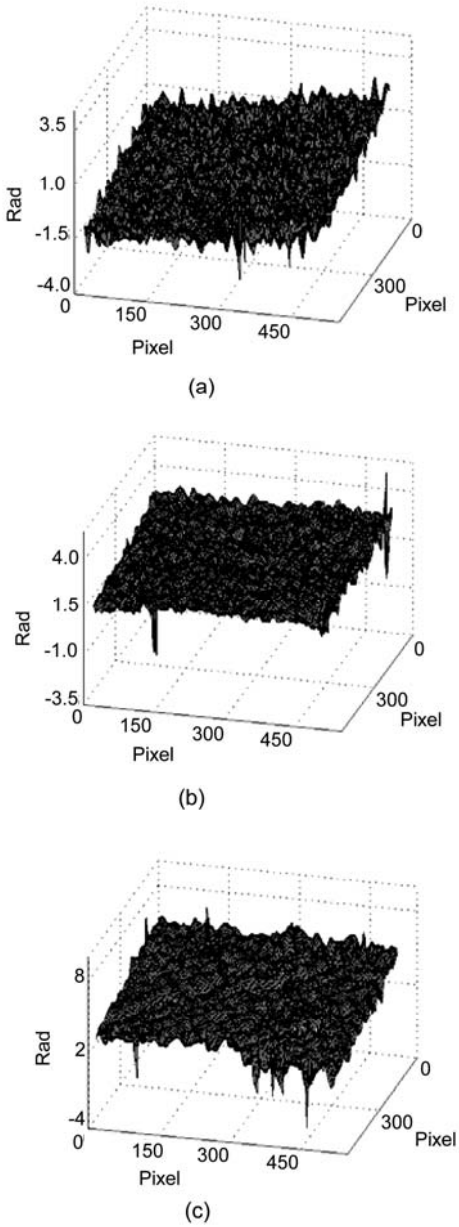


**Fig. 6 3D images for the concrete surface. (a) #2; (b) #3; (c) #4**

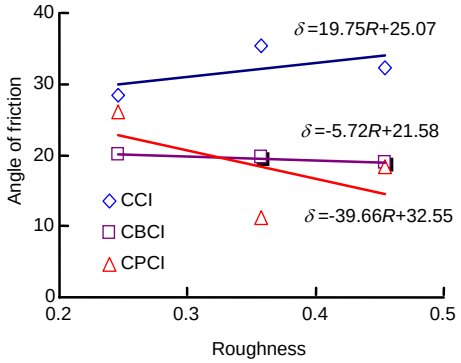


**Fig. 7 Angle of friction vs. roughness $R_{max}$/10 for CCI, CBCI and CPCI**

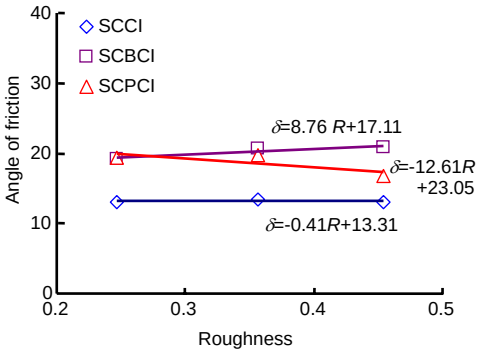


**Fig. 9 Angle of friction vs. roughness $R_{max}$/10 for SCCI, SCBCI and SCPCI**

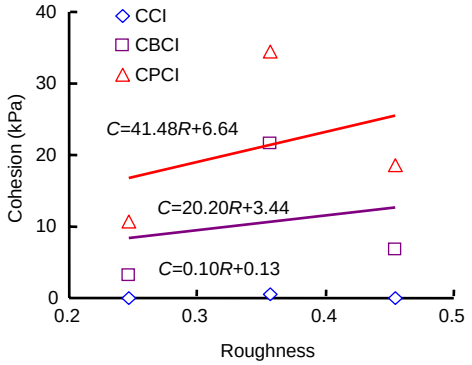


**Fig. 8 Cohesion vs. roughness $R_{max}$/10 for CCI, CBCI and CPCI**

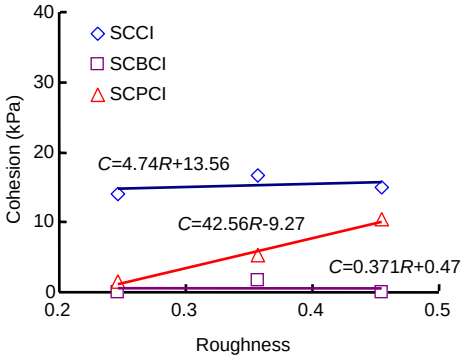


**Fig. 10 Cohesion vs roughness $R_{max}$/10 for SCCI, SCBCI and SCPCI**

The angle of friction for SCCI decreases by 0.41$R$ and the angle of friction for SCBCI increases by 8.76$R$. The angle of friction for SCPCI decreases by 12.61$R$ (Fig. 9). Cohesion increases with roughness. It increases by 4.74$R$ for SCCI, slightly decreases by 0.37$R$ for SCBCI, and decreases by 42.56$R$ for SCPCI (Fig. 10). The cohesion increases dramatically when using polymer as an interface layer between sandy clay compared to cohesion of SCCI. Using bentonite as an interface layer between sandy clay and concrete shows contrast results. It increases the cohesion also, but the increase is small compared to both SCCI and SCPCI.

### 3.5 Sliding ratio

Inspecting the simple shear tests and relation of sliding displacement vs. deformation displacement reveals two types of failure: (1) sliding failure and (2) deformation failure. Sliding failure occurs when the sample continues in sliding until failure. Deformation failure occurs when the deformation displacement ($d_d$) continues until failure. Increasing the sliding displacement during the simple shear test may be related to inefficient concrete surface shape, which augments the interfacial shear strength. It also may be related to high shear strength of the soil sample.

Based on the relation between sliding displacement and deformation displacement, we could define a parameter used to recognize between the two types of failure above-mentioned. Sliding ratio ($S_r$) presents the ratio of sliding displacement to the total displacement:

$$S_r = \frac{d_s}{d_s + d_d}, \tag{1}$$

where $S_r$ is the sliding ratio, $d_s$ is the sliding displacement, and $d_d$ is the deformation displacement.

The sliding ratio varies between zero and one. Zero means the sample deforms without sliding and one means the sample slides without deformation. Sliding failure manifests a sliding ratio ($S_r$) greater than 0.5, while deformation failure manifests a sliding ratio ($S_r$) less than 0.5.

Except in the case of CCI, the average sliding ratio ($S_r^{av}$) shows a magnitude less than 0.5 (Tables 5 and 6). The case CCI reveals the largest amount of the average sliding ratio ($S_r^{av}$), which is equal to 0.75. This magnitude confirms occurrence sliding failure because it is greater than 0.5. Polymer slurry as an interface layer between clay and concrete (CPCI) reduces the average sliding ratio ($S_r^{av}$) to 0.45. Bentonite slurry also reduces the average sliding ratio to 0.38. Polymer and bentonite increase the cohesion from 0.5 for CCI to 9.0 for CBCI and 14 for CPCI causing the sample to deform until failure. They increase the bond between clay and concrete, then decrease sliding compared to the case of CCI.

SCCI has the lowest magnitude of average sliding ratio ($S_r^{av}$), 0.25 (Table 6). Using bentonite slurry as an interface layer between soil and concrete (SCBCI) increases the sliding ratio to 0.36 and using polymer slurry as an interface layer between soil and concrete (SCPCI) increases the average sliding ratio to 0.39. Bentonite and polymer increase sliding, and may act as a lubricant between concrete and sandy clay. Failure by deformation, however, still occurs because the average sliding ratio is less than 0.5.

**Table 5 Average sliding ratio for CCI, CBCI and CPCI**

| Concrete type | $S_r$ | | |
|---|---|---|---|
| | CCI | CBCI | CPCI |
| #1 | 0.77 | 0.26 | 0.44 |
| #2 | 0.98 | 0.93 | 0.59 |
| #3 | 0.86 | 0.28 | 0.31 |
| #4 | 0.57 | 0.20 | 0.48 |
| #5 | 0.56 | 0.23 | 0.44 |
| av. | 0.75 | 0.38 | 0.45 |

**Table 6 Average sliding ratio for SCCI, SCBCI and SCPCI**

| Concrete type | $S_r$ | | |
|---|---|---|---|
| | SCCI | SCBCI | SCPCI |
| #1 | 0.19 | 0.24 | 0.43 |
| #2 | 0.38 | 0.65 | 0.39 |
| #3 | 0.25 | 0.35 | 0.41 |
| #4 | 0.17 | 0.17 | 0.27 |
| #5 | 0.27 | 0.38 | 0.44 |
| av. | 0.25 | 0.36 | 0.39 |

### 3.5.1 Sliding and deformation shear stress

Based on the proposed sliding ratio, multiplying the applied shear stress by the sliding ratio gives the sliding shear stress (Eq. (2)). Subtracting sliding shear stress from the applied shear stress gives the deformation shear stress (Eq. (3)).

$$\tau_s=\tau_t S_r, \tag{2}$$

$$\tau_d=\tau_t-\tau_s, \tag{3}$$

where $\tau_s$ is the sliding shear stress, $\tau_d$ is the deformation shear stress and $\tau_t$ is the total shear stress.

Total shear displacement is also divided into sliding displacement and deformation displacement. They can be measured directly through carrying out a simple shear test.

$$d_t=d_s+d_d, \tag{4}$$

where $d_t$ is the total displacement, $d_s$ is the sliding displacement and $d_d$ is the deformation displacement. The relations of $\tau_s$ vs. $d_s$ and $\tau_d$ vs. $d_d$ show nearly the same hyperbolic shape that was seen with $\tau$ vs. $d_t$ (Figs. 11 and 12). The graphs represent the results obtained by performing the simple shear test on SCBCI (#3). These two figures show the failure characteristics of contact between soil and concrete as well as the failure characteristics of soil sample. They represent the sliding and deformation characteristics of the sample during the test.

### 3.5.2 Sliding and deformation parameters

Applied shear stress is distributed to sliding shear stress (which causes sliding displacement), and deformation shear stress (which causes deformation displacement). Relations of sliding shear stress vs. sliding displacement and deformation shear stress vs. deformation displacement are shown in Figs. 11 and 12.

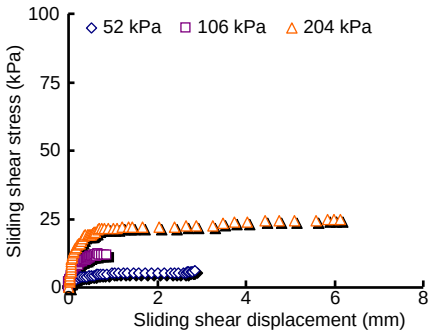


**Fig. 11 $\tau_s$ vs. $d_s$ for SCBCI, concrete #3**

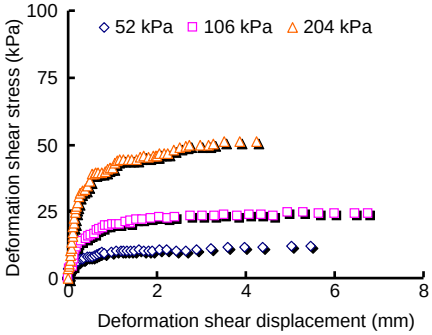


**Fig. 12 $\tau_d$ vs. $d_d$ for SCBCI, concrete #3**

Maximum sliding shear stress ($\tau_s$) vs. normal stress ($\sigma_n$) has a linear response. The slope of the linear relation of $\tau_s$ vs. $\sigma_n$ gives the angle of sliding $\delta_s$, and the threshold gives the cohesion $C_s$ (Fig. 13). The angle of deformation ($\delta_d$) represents the slope of linear relation of maximum deformation shear stress $\tau_d$ vs. normal stress $\sigma_n$ and $C_d$ represents the cohesion of the soil.

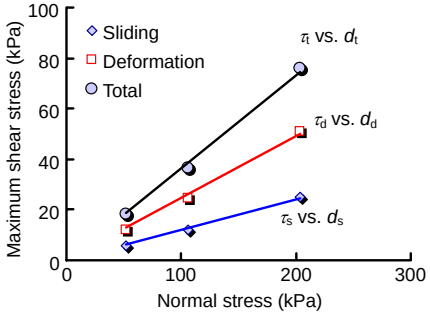


**Fig. 13 Maximum shear stress vs. normal stress for SCBCI, concrete #3**

Tables 7 to 10 show the sliding angle and deformation angle for all groups. The sliding angles ($\delta_s$) and deformation angles ($\delta_d$) are coherent with the sliding ratio ($S_r$). For instance, the lowest average sliding angle ($\delta_s^{av}$) that was calculated for SCCI is 3.27° and superlative sliding angle for CCI is 23.16° (Tables 7 and 9). This is compatible with the sliding ratio, where $S_r^{av}$ for SCCI equals 0.25 and the greatest $S_r^{av}$ is for CCI, which is equal to 0.75. The larger the sliding angle, the larger sliding ratio, and vice versa. The data suggest a precise failure formula which can make use of the sliding ratio derived from the sliding-deformation relationships. The failure formula considers the sliding parameters ($\delta_s$, $C_s$) and the deformation parameters ($\delta_d$, $C_d$). Beginning from the reality that total magnitude of shear stress equals to sliding shear stress plus deformation shear stress:

$$\tau_t=\tau_s+\tau_d. \quad (5)$$

Since $\tau_s=\sigma_n \tan \delta_s$ and $\tau_d=\sigma_n \tan \delta_d$, the failure equation

**Table 7 Sliding angle and sliding cohesion for CCI, CBCI and CPCI**

| Concrete type | $C$ | | | $\delta$ (°) | | |
|---|---|---|---|---|---|---|
| | CCI | CBCI | CPCI | CCI | CBCI | CPCI |
| #1 | 0.5 | 0.0 | 0.0 | 20.5 | 4.1 | 10.7 |
| #2 | 0.0 | 3.1 | 6.4 | 28.0 | 18.8 | 15.4 |
| #3 | 0.0 | 1.9 | 5.8 | 27.7 | 5.2 | 5.8 |
| #4 | 0.3 | 4.2 | 16.3 | 20.3 | 3.9 | 5.4 |
| #5 | 0.8 | 3.1 | 2.7 | 19.3 | 8.4 | 6.6 |
| av. | 0.3 | 2.5 | 6.3 | 23.2 | 8.1 | 8.8 |

**Table 8 Deformation angle and deformation cohesion for CCI, CBCI and CPCI**

| Concrete type | $C$ | | | $\delta$ (°) | | |
|---|---|---|---|---|---|---|
| | CCI | CBCI | CPCI | CCI | CBCI | CPCI |
| #1 | 0.2 | 0.0 | 0.0 | 0.3 | 11.8 | 13.5 |
| #2 | 0.0 | 0.2 | 4.4 | 0.4 | 1.3 | 10.7 |
| #3 | 0.0 | 4.9 | 12.8 | 4.6 | 13.7 | 12.6 |
| #4 | 0.2 | 17.4 | 18.1 | 15.1 | 15.8 | 5.9 |
| #5 | 0.6 | 10.4 | 3.4 | 6.5 | 13.8 | 8.0 |
| av. | 0.2 | 6.6 | 7.7 | 5.3 | 11.3 | 10.1 |

**Table 9 Sliding angle and sliding cohesion for SCCI, SCBCI and SCPCI**

| Concrete type | $C$ | | | $\delta$ (°) | | |
|---|---|---|---|---|---|---|
| | SCCI | SCBCI | SCPCI | SCCI | SCBCI | SCPCI |
| #1 | 0.9 | 0.0 | 2.8 | 2.7 | 4.8 | 8.3 |
| #2 | 5.3 | 0.0 | 0.6 | 5.0 | 12.3 | 7.5 |
| #3 | 3.8 | 0.0 | 4.2 | 3.3 | 7.3 | 6.8 |
| #4 | 2.8 | 0.3 | 1.4 | 2.3 | 3.5 | 5.4 |
| #5 | 3.8 | 0.0 | 2.7 | 3.1 | 7.9 | 6.6 |
| av. | 3.3 | 0.1 | 2.3 | 3.3 | 7.2 | 7.0 |

**Table 10 Deformation angle and deformation cohesion for SCCI, SCBCI and SCPCI**

| Concrete type | $C$ | | | $\delta$ (°) | | |
|---|---|---|---|---|---|---|
| | SCCI | SCBCI | SCPCI | SCCI | SCBCI | SCPCI |
| #1 | 3.6 | 0.0 | 3.8 | 11.5 | 15.1 | 11.1 |
| #2 | 8.8 | 0.0 | 0.9 | 8.2 | 6.8 | 11.9 |
| #3 | 11.2 | 0.0 | 6.2 | 9.7 | 13.6 | 9.9 |
| #4 | 13.8 | 0.3 | 3.9 | 11.2 | 3.5 | 14.3 |
| #5 | 1.5 | 0.0 | 3.4 | 12.9 | 7.9 | 8.2 |
| av. | 9.7 | 0.3 | 3.7 | 9.7 | 13.0 | 11.0 |

will be expressed as

$$\tau_t=C_s+\sigma_n\tan\delta_s+C_d+\sigma_n\tan\delta_d. \quad (6)$$

Eq. (6) requires evaluating four parameters: cohesion and angle of friction for contact, and cohesion and angle of deformation for the soil. These can be computed from the simple shear apparatus with the aid of the sliding ratio proposed in this study.

## 4 Conclusion

This study used simple shear tests to explore the effect of using thin layers of bentonite and polymer between soil and concrete on the interfacial shear strength. Five specimens of concrete with different surface shapes were used with two types of soil: clay and sandy clay. The following conclusions were obtained:

1. Using bentonite slurry as an interface layer (1–2 mm) between clay and concrete reduces the interfacial shear strength by 23% and using bentonite slurry as an interface layer (1–2 mm) between sandy clay and concrete increases the interfacial shear strength by 10%.

2. Using polymer slurry as an interface layer between clay and concrete decreases the interfacial shear strength by 17% and using polymer as an interface layer between sandy clay and concrete increases the interfacial shear strength by 10%. Using bentonite and polymer slurry as an interface layer between clay and concrete decreases the sliding ratio by 50%–60% while increasing the sliding ratio to 44%–56% when used as an interface layer between sandy clay and concrete.

## Acknowledgments

The Er-Tan Hydraulic-power Limited Company is appreciated. The authors also would like to thank Dr. Fu-jun YANG, South East University, China for assistance in performing the experiments on concrete roughness.

## References

Ata, A., O'Neill, M., 2000. The physicochemical interaction between PHPA polymer slurry and cement mortar. *Geotechnical Testing Journal*, **23**(2):225-235. [doi:10.1520/GTJ11047J]

Barla, G., Barla, M., Camusso, M., Martinotti, M.E., 2007 Setting up a New Direct Shear Testing Apparatus. The Second Half Century of Rock Mechanics, 11th Congress of the International Society for Rock Mechanics, Lisbon, **1**:415-418.

Brown, D., 2002. Effect of construction on axial capacity of drilled foundations in piedmont soils. *Journal of Geotechnical and Geoenvironmental Engineering*, **128**(12): 967-973. [doi:10.1061/(ASCE)1090-0241(2002)128:12(967)]

Camp, W.M., Brown, D.A., Mayna, P.W., 2002. Construction Methods Effects on Drilled Shaft Axial Performance. Proceedings of the International Deep Foundations Congress, Reston, USA, p.193-208. [doi:10.1061/40601(256)14]

Cernak, B., 1973. The Time Effect of Suspension on the Behavior of Piers. Proceedings of Sixth European Conference on Soil Mechanics and Foundation Engineering, Vienna, Austria, p.111-114.

Holden, J.C., 1984. Construction of Bored Piles in Weather Rock, Part 4: Bentonite Construction Procedures. Technical Report No. 6, Road Construction Authority of Victoria, Australia.

Huang, L., Qian, K.M., Pan, B., Asundi, A.K., 2009. Comparison of Fourier transform, windowed Fourier transform, and wavelet transform methods for phase extraction from a single fringe pattern in fringe projection profilometry. *Optics and Lasers in Engineering*, **48**(2):141-148. [doi:10.1016/j.optlaseng.2009.04.003]

Jeong, S., Ahn, S., Seol, H., 2009. Shear load transfer characteristics of drilled shafts socketed in rocks. *Rock Mechanics and Rock Engineering*. [doi:10.1007/s00603-009-0026-4]

Kheng, H.W., 1989. Rheological and Physico-chemical Properties of Palygorskite and Anionic Polyacrylamide Polymer Slurries Used in Drilled Shaft Construction. PhD Thesis, University of Florida, Gainsville, USA.

Majano, R.E., O'Neill, M.W., 1993. Effect of Mineral and Polymer Slurries on Perimeter Load Transfer in Drilled Shafts. A Report to ADSC: The International Association of Foundation Drilling, University of Houston.

Majano, R.E., O'Neill, M.W., Hassan, K.M., 1994. Perimeter load transfer in model drilled shafts formed under slurry. *Journal of Geotechnical Engineering, ASCE*, **120**(12):2136-2154. [doi:10.1061/(ASCE)0733-9410(1994)120:12(2136)]

Nash, K.L., 1974. Stability of trenches filled with fluids. *Journal of the Construction Engineering Division, American Society of Civil Engineers*, **100**(4):533-542.

O'Neill, M.W., Hassan, K.H., 1994. Drilled Shafts: Effects of Construction on Performance and Design Criteria. Proceedings International Conference on Design and Construction of Deep Foundations, U.S. Federal Highway Administration, **1**:137-187.

O'Neill, M.W., Reese, L.C., 1999. Drilled shafts: Construction

Procedures and Design Methods. The International Association of Foundation Drilling, Publication No. ADSC-TL4, Vol. I.

Pells, P.J.N., Douglas, D.J., Rodway, B., Thorne, C., McMahon, B.K., 1978. Design loadings for foundations in shale and sandstone in the Sydney Region. *Australian Geomechanics Journal*, **2**:31-38.

Reddy, E.S., Chapman, D.N., Saatry, V., 2000. Direct shear interface test for shaft capacity of piles in sand. *Geotechnical Testing Journal*, **23**(2):199-205. [doi:10.1520/GTJ11044J]

Shakir, R.R., Zhu, J.G., 2009. Behavior of compacted clay concrete interface. *Frontiers of Architecture and Civil Engineering in China*, **3**(1):85-92. [doi:10.1007/s11709-009-0013-6]

Takeda, M., Mutoh, K., 1983. Fourier transform profilometry for the automatic measurement of 3-D object shapes. *Applied Optics*, **22**(24):3977-3982. [doi:10.1364/AO.22.003977]

Tsubakihara, Y., Kisheda, H., Nishiyama, T., 1993. Friction between cohesive soils and steel. *Soils and Foundations*, **33**(2):145-156.

Tucker, K.L., Reese, L.C., 1984. The Effect of Bentonitic Slurry on Drilled Shafts. Center for Transportation Research, University of Texas, Austin, USA.

Uesugi, M., Kishida, H., Uchikawa, Y., 1990. Friction between dry sand and concrete under monotonic and repeated loading. *Soils and Foundations*, **30**(1):115-128.

Wang, W., Lu, T.H., 2007. Modeling Experiment on Interface Shearing Behavior between Concrete and Unsaturated Soil with Various Degrees of Saturation. *In:* Yin, Z.Z., Yuan, J.P., Chiu, A.C.F. (Eds.), Proceeding of the 3rd Asian Conference on Unsaturated soils, Nanjing, China. Science Press, Beijing, p.315-318.

Wates, J.A., Knight, K., 1975. The Effect of Bentonite on the Skin Friction in Cast-in-place Pile and Depth Ram Walls. Proceedings of Sixth Regional Conference for Africa on Soil Mechanics and Foundation Engineering, Durban, South Africa, p.183-188.

Xue, F.G., Seidel, J.P., Haberfield, C.M., Bouazza, A., 2005. Wear of Sandstone Surfaces during Direct Shear Testing of Sandstone/Concrete Joints. Advances in Deep Foundations (GSP 132) Part of Geo-Frontiers Proceedings of the Sessions of the Geo-Frontiers Congress, Austin, Texas, USA. [doi:10.1061/40778(157)9]

Yin, Z.Z., Zhu, H., Xu, G.H., 1995. A study of deformation in the interface between soil and concrete. *Computers and Geotechnics*, **17**(1):75-92. [doi:10.1016/0266-352X(95)91303-L]

Zhang, B., Fu, J., Yu, Y., Hu, L., 2008. Simple shear test for interfaces between core and filter soils in rock-fill dams. *Geotechnical Testing Journal*, **31**(3):252-260. [doi:10.1520/GTJ100859]

Zhang, G., Zhang, J.M., 2009. Numerical modeling of soil-structure interface of a concrete-faced rockfill dam. *Computer and Geotechnics*, **36**(5):762-772. [doi:10.1016/j.compgeo.2009.01.002]

Zhu, J.G., Yin, J.H., 2001. Drained creep behaviour of soft Hong Kong marine deposits. *Geotechnique*, **51**(5):471-474. [doi:10.1680/geot.51.5.471.39978]